Research Article

Strengthening Effect of Prestressed Near-Surface-Mounted CFRP Tendon on Reinforced Concrete Beam

Woo-Tai Jung [ID], **Jong-Sup Park** [ID], **Jae-Yoon Kang** [ID], **and Hee Beom Park** [ID]

Department of Infrastructure Safety Research, Korea Institute of Civil Engineering and Building Technology, Goyang-Si, Republic of Korea

Correspondence should be addressed to Hee Beom Park; heebeompark@kict.re.kr

Efforts are being made to use FRP (fiber-reinforced polymer) for reinforcements instead of traditional construction materials like steel owing to its remarkable mechanical properties. Among them, this study developed a CFRP tendon to be used as near-surface-mounted reinforcement together with a dedicated prestressing system and investigates experimentally the strengthening effect considering various variables including the amount of reinforcement, the bond performance, and the strength and damage ratio of the concrete. The test results reveal that one line of reinforcement improved the strengthening performance by about 55% and two lines by 96% and that the bonding of the CFRP tendon enhanced the strengthening performance by 15%. Higher strength and damage of the concrete seem to have a poor effect on the overall strengthening performance. However, the use of CFRP tendon with bond performance higher than 11 MPa, filler, and anchorage system appears to promote stable strengthening behavior.

1. Introduction

Owing to its remarkable mechanical properties, FRP (fiber-reinforced polymer) was first adopted by the aerospace industry and is today extensively applied from the sport industry to the manufacturing of automobile parts or as construction material. Being lighter than steel and offering higher mechanical properties, FRP actually is well emerged as a replacement of steel in various sectors. Steel and concrete are traditional materials that have been used historically in the construction industry. However, the diversification and enlargement of built structures make them heavier, and there is also the corrosion problem of steel. Accordingly, efforts are being made to employ FRP instead of steel. This tendency is particularly marked in bridge engineering where FRP is continuously developed and applied to replace steel for reinforcement and tendon [1].

A wide variety of FRP tendons are produced according to the type of fiber and resin, size, and shape. Since the tendon must sustain permanent loading, carbon fiber or aramid fiber can be applied rather than glass fiber in view of the resistance to creep [2]. Consequently, the FRP tendon is fabricated using carbon fiber (CFRP) or aramid fiber (AFRP) and produced with round cross sections similarly to the conventional steel tendon. FRP sheets were also developed because FRP was first exploited for strengthening purpose in the construction sector. To date, the commercialized products are Leadline™, CFCC, and Aslan™ 200 for CFRP tendons and Parafil®, Technora®, and FiBRA for AFRP tendons. In the case of FRP sheets, those using CFRP are CaborDur® and CFK and those using AFRP are Arapree®. Korea started to show keen interest on FRP tendons since 2000s and developed the KICT tendon. At the exception of Technora® which uses vinylester resin, most of the FRP tendons adopt epoxy resin [1].

The conventional anchor for steel strands, which compresses them physically, cannot be used for the FRP tendon because of its low transverse strength. This situation led to the proposal of special anchors for the commercially available FRP tendon products. Nanni et al. [3] evaluated the anchoring performance of 10 different FRP anchors by classifying them into wedge type, potted type, and spike type instead of the 6 types specified by ACI [4] that are clamp type, plug-and-cone type, straight sleeve type, contoured

sleeve type, metal overlay type, and wedge type. Other studies related to the anchors for FRP tendon classified them into clamp type, swaged type, spike type, sleeve type, and wedge type [5, 6].

The externally bonded reinforcement (EBR) is often cited as the most popular strengthening method using FRP. However, the existing EBR of FRP experienced bond failure and developed a poor strengthening affect at service load, which led recently to the proposal of new methods introducing prestress by means of FRP [7]. Even if the use of FRP tendons leads to numerous advantages, there are still problems including the achievement of effective anchoring considering the material characteristics of FRP or the prestressing of the FRP tendon. The pre- or post-tensioning of the FRP tendon necessitates not only special anchoring device but also a fitted prestressing system. The construction sector is still now developing active methods for the prestress of deteriorated structures [8–10]. Among the strengthening methods, the prestressed near-surface-mounted reinforcement (NSMR) combines the advantages of both NSMR and prestressing. Its application enables to improve the serviceability as well as to exploit efficiently the FRP tendon. However, this method requires a special anchor different from that used in prestressed concrete (PSC) structures to embed the tensioned FRP tendon in the concrete surface. The anchor for prestressed NSMR can be classified into indirect and direct methods with respect to the way in which the tensioning frame is installed. The indirect method resembles the pre-tensioning of PSC structures and uses a separate reaction frame for tensioning the FRP tendon. Many researchers adopt this method for its convenience but it is inadequate for on-site application. The direct method resembles the post-tensioning of PSC structures and uses the structure to be strengthened as reaction frame.

For the prestressed NSMR, this study developed a practical prestressing system and a swaged-type anchor enabling to exploit more than 60% of the tensile strength of the CFRP tendon. The loading test is conducted to examine the strengthening performance of the developed method considering diversified variables, and the experimental results are validated analytically.

2. CFRP Tendon

The commercialized FRP tendons are fabricated mainly by fiber manufacturers or companies that formerly supplied steel strands. Recently, companies specialized in FRP fabrication have also entered in the FRP tendon market. Tables 1 and 2 list the major AFRP and CFRP tendons currently commercially available. The values indicated in the tables are those provided in the homepage of the supplier or found in the references when unavailable.

Compared to the CFRP tendons, the AFRP tendons develop similar or higher rupture strain but lower tensile strength and elastic modulus and rather unfavorable relaxation characteristics. Besides, owing to the strong resistance to shock characterizing the aramid fiber, Parafil® is used as a tendon even without being coupled with resin.

Since the bond strength indicating the bond characteristics between concrete and the tendon is more influenced by the cross-sectional shape of the tendon than by the type of fiber, the cross-sectional shape of the FRP tendon is worked through various treatments to improve the bond performance like sand coating or by indenting or deforming its surface. Other tendons are also made by twisting to resemble the prestressing strand.

This study fabricated new CFRP tendons with good relaxation characteristics. With a diameter of 10 mm, using epoxy as resin and fiber volume ratio of 65%, the tendon develops tensile strength and elastic modulus larger than 3,000 MPa and 170 GPa, respectively. The tendon was fabricated to present round sections, and aluminum oxide coating was applied as shown in Figure 1 to enhance the bond performance. This treatment secured the bond strength of about 11 MPa. Figures 2 and 3 show the tensile test of the CFRP tendon and images of the rupture of the CFRP tendon.

3. Anchor and Prestressing System for CFRP Tendon

3.1. Anchor for CFRP Tendon. Jung et al. [6] proposed the wedge-, bond-, and swaged-type anchors shown in Table 3 for the CFRP tendon.

The swaged-type anchor presents smaller size than the wedge-type or bond-type anchor but needs to pay attention on the swage pressure brought by the change in the inner and outer diameters of the sleeve and the stress concentration occurring at the end of the sleeve in order to improve the anchoring performance (Table 3). Since the size of the anchor must be reduced as possible to apply the prestressed NSMR, analytical and experimental studies were conducted to derive the dimensions of the swaged-type anchor for the CFRP tendon [6]. These studies enabled to achieve anchoring performance higher than 60% of the tensile resistance of the CFRP tendon. The length and diameter of the swaged-type anchor before swaging are, respectively, 135 mm and 25.9 mm but become 155 mm and 24 mm after swaging through the occurrence of plastic deformation, which generates the swage force on the surface of the CFRP tendon.

3.2. Prestressing System for CFRP Tendon. A special prestressing system is necessary for prestressing the structure by NSMR. The previous systems can be classified into indirect and direct methods with respect to the way in which the tensioning frame is installed as shown in Figure 4. In the prestressed NSMR by the indirect method, the structure (concrete beam) to be strengthened is disposed on a separate tensile reaction frame, and grooves are indented in the surface of the structure prior to the tensioning of the FRP tendon and the filling of the grooves (Figure 4). Numerous researchers who studied the prestressed NSMR exploited such an indirect method. The anchoring device using the closed-frame shown in Figure 5 can also be classified as pertaining to the indirect method [7]. However, the need of a

TABLE 1: Commercialized AFRP tendons.

Characteristics	Arapree®	FiBRA	Technora®	Parafil®
Fiber	Twaron	Kevlar49	Technora	Kevlar49
Resin	Epoxy	Epoxy	Vinylester	Vinylester
Fiber volume ratio	0.45	0.65	0.65	1.00
Tensile strength (GPa)	1.21	1.11	1.9	1.2–1.9
Elastic modulus (MPa)	501	68.61	53	71–125.81
Bond strength (MPa)	7.7	10–13	10–16	—
Max. strain (%)	2.31	1.61	3.6	1.5–3.51
Thermal exp. coeff. ($\times 10^{-6}$)	−2	−2	−3	—
Relaxation (%)	11–14	12	11.6	6–91
Supplier	Sireg (Italy)	FiBEX Co. (Japan)	Teijin (Japan)	Linear Composites (UK)
Reference		[4]	[4, 11]	[4]

TABLE 2: Commercialized CFRP tendons.

Characteristics	Leadline™	CFCC	Carbon-Stress®	Carbopree®	Aslan200	CarboDur®	CFK
Fiber	Carbon	Carbon	Carbon	Carbon	Carbon	Carbon	Carbon
Resin	Epoxy	Epoxy	Epoxy	Epoxy	Epoxy	Epoxy	Epoxy
Fiber volume ratio	0.65	0.65	0.65	—	—	0.68	—
Tensile strength (GPa)	2.25–2.55	2.69	2.7	2.3	2.1–2.2	2.8	1.3–2.05
Elastic modulus (MPa)	142–150	155	158.8	130	124	160	165–210
Bond strength (MPa)	4–20	7–11	—	13.7	8.45	—	—
Max. Strain (%)	1.3–1.5	1.7	1.7	1.8	1.67–1.81	1.69	1.56
Thermal exp. coeff. ($\times 10^{-6}$)	−0.9	0.6	2	—	−9	—	—
Relaxation (%)	2–3	1.3	1	—	Negligible	—	—
Supplier	Mitsubishi Plastics Infratec Co. (Japan)	Tokyo Rope (Japan)	Nedri (Netherlands)	Sireg (Italy)	Hughes Brothers (USA)	SIKA (Swiss)	S&P (Swiss)
Reference	[4]		[12]	[13]	—	—	—

separate tensile reaction frame restrains strongly its actual application on site.

In the direct-type anchoring device, the structure to be strengthened is exploited as tensile reaction frame. Numerous researchers adopted this method to install the tensioning device at the end of the concrete beam. Figure 6 illustrates the realization of the prestressed NSMR of a beam using the clamped-type anchor and the direct-type anchoring device. Unlike the indirect method, compressive force applies on the concrete beam during the tensioning of FRP. This type of anchor cannot be applied on-site in its present form. Figure 6 presents the details of the fixed end and the tensioned end of the anchoring device used in the fabrication of prestressed NSMR beam by Badawi [14].

Since it is generally difficult to access to the end of the beam on-site, the anchor shown above is inapplicable [15]. Accordingly, a research team of Lecce University in Italy proposed the anchoring device shown in Figure 7, which allows tensioning from the bottom of the structure [7].

A research team of Calgary University developed the direct tensioning device composed of one temporary anchor and one permanent anchor shown in Figure 8 to execute tensioning from the concrete bottom [7]. The movable bracket and fixed bracket in Figure 8 are temporary

structures installed for the tensioning that are removed after completion of the tensioning work. The steel anchor installed at the tensioned end is movable during tensioning but is fixed to concrete after completion of the work.

For the prestressed NSMR, the Korea Institute of Construction & Building Technology (KICT) developed a new tensioning system using the fixed anchor installed in the concrete beam as tensile reaction frame (Figure 9) [1]. Unlike that of Calgary University, the direct-type anchor of KICT employs the permanent anchor fixed in concrete as tensile reaction frame and fixes the tensioned FRP tendon on this permanent anchor by means of a nut. This disposition enables to minimize additional damage of the member that would occur to install the device. Moreover, spatial efficiency is also secured because tensioning is executed at the front of the anchor.

4. Test for Strengthening Performance of Prestressed NSMR

NSMR proceeds by embedding the FRP tendon in a groove prepared in advance and covering it by means of high-strength epoxy or grout. Unlike EBR, NSMR does not need to prepare the surface. Its applicability depends on the

(a)   (b)
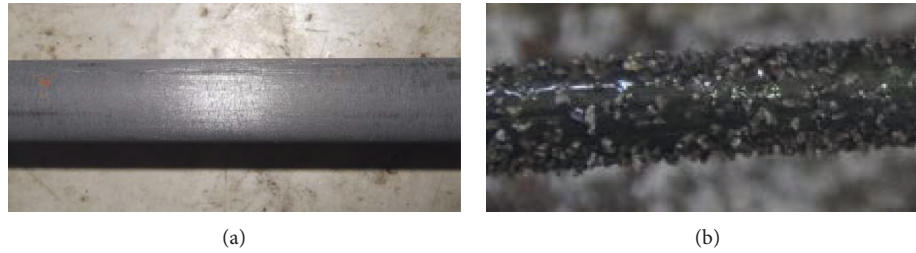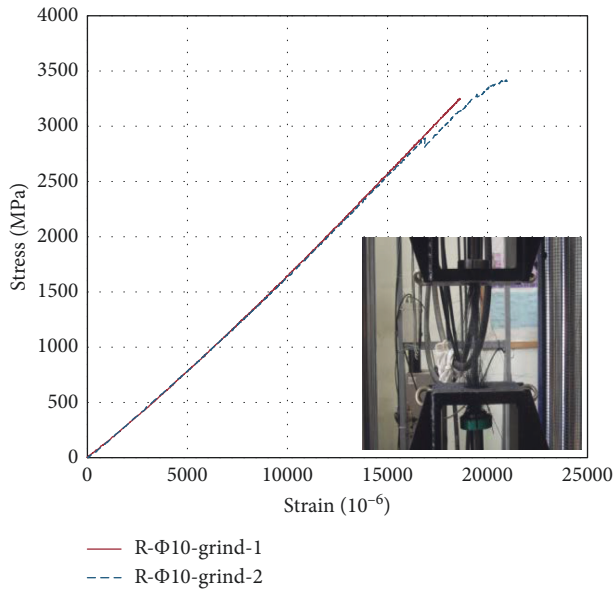
FIGURE 1: Surface treatment of CFRP tendon.

FIGURE 2: Results of tensile test.

FIGURE 3: Rupture of CFRP tendon.

concrete cover and the embedded FRP tendon can be protected from external damage [16]. Studies on NSMR mostly focused on the strengthening effect and bond characteristics and recently try to introduce prestress in the NSMR tendon.

The present study conducts prestressed NSMR using a newly developed tensioning system and intends to examine the flexural rigidity with respect to diversified variables. As shown in Figure 10, the specimens made of 40 MPa concrete are 6,400 mm-long with a rectangular cross section of height and width 600 mm and 400 mm, respectively. All the specimens are fabricated with the same cross-sectional dimensions to observe the improvement of the performance according to the sele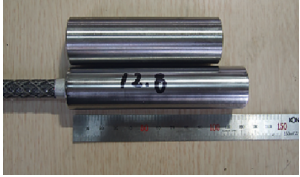cted variables. The test is performed on two groups of specimens. The first group (I) is intended to examine the basic strengthening performance of the prestressed NSMR by considering the amount of reinforcement and surface treatment of the CFRP tendon as variables in comparison with the nonstrengthened reference specimen (Control-1). The second group (II) is intended for the evaluation of the strengthening effect considering the matrix concrete strength, the extent of concrete damage, and the eventual bonding of the tendon as variables.

4.1. Test Variables. The designation of the specimen is explained in Figure 11 with respect to the variables. The first character designates the type of filler with M for mortar and E for epoxy. The second string of character indicates the surface treatment of the FRP tendon with OX for oxide coating, SC for sand coating, and GR for grind. The third string of character indicates the number of FRP tendons (1 for 1 line of reinforcement; 2 for 2 lines of reinforcement). The fourth string of character stands for the eventual bonding between the filler and the concrete with B for bond and UB for unbond. The fifth string of character indicates the concrete strength (40 MPa). The sixth and last string of character designates the damage ratio of the concrete (strength of 30% or 60% with respect to the ultimate strength of the Control specimen). Damage was provoked by preliminary 4-point loading of the undamaged specimen up to a load corresponding to 30% or 60% of the ultimate strength of the Control specimen. All the strengthened specimens applied the same developed length of 4,800 mm for the CFRP tendon. Table 4 lists the adopted specimens with their designation according to the test variables.

4.2. CFRP Tendon. The CFRP tendon used for the strengthening of the specimens has a diameter of 10 mm and presents the physical properties listed in Table 5. The allowable tension force to be introduced in the proposed prestressed NSMR is set to be below 60% of the strength of the tendon. Accordingly, the tension force of 100 kN corresponding to about 40% of the 240 kN tensile strength of the FRP tendon was applied in the fabrication of the specimens.

A total of 3 variables related to the shape and surface treatment of the CFRP tendon were considered in the fabrication of the tendon to be used in the specimens. Table 6 lists the types of surface treatment applied to achieve the CFRP tendons. These treatments are grinding, sand coating, and oxide coating.

TABLE 3: Types of anchor for CFRP tendon.

Anchor type	Wedge	Bond	Swaged
Image			
Characteristics	Shortest anchor length Wedge stress concentration	Need sufficient anchor length Low-cost fabrication possible Remarkable adaptability to change of the diameter of tendon	Possibility to shorten the anchor length High fabrication cost Need for special equipment
Anchor length	60 mm (except sleeve length)	400 mm	150 mm (after compression)

(a)

(b)
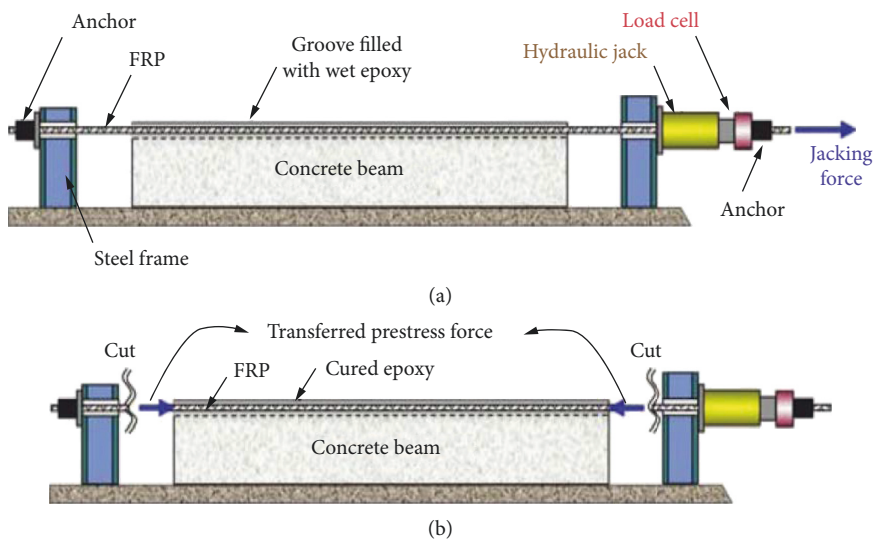
FIGURE 4: Anchoring by indirect method [7].
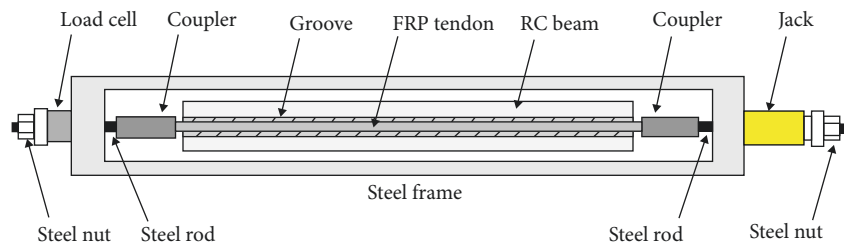
FIGURE 5: Indirect anchoring using closed-frame [7].
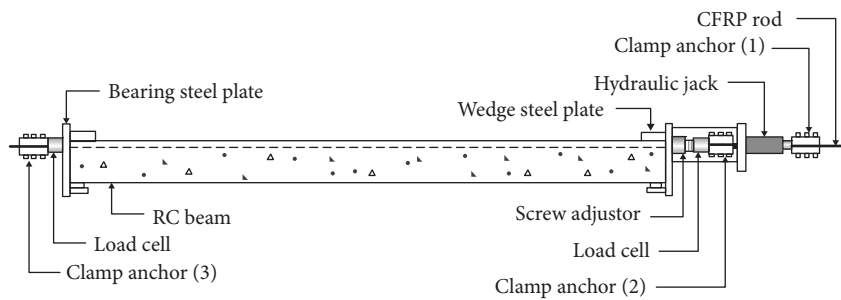
FIGURE 6: Anchoring by direct method [14].
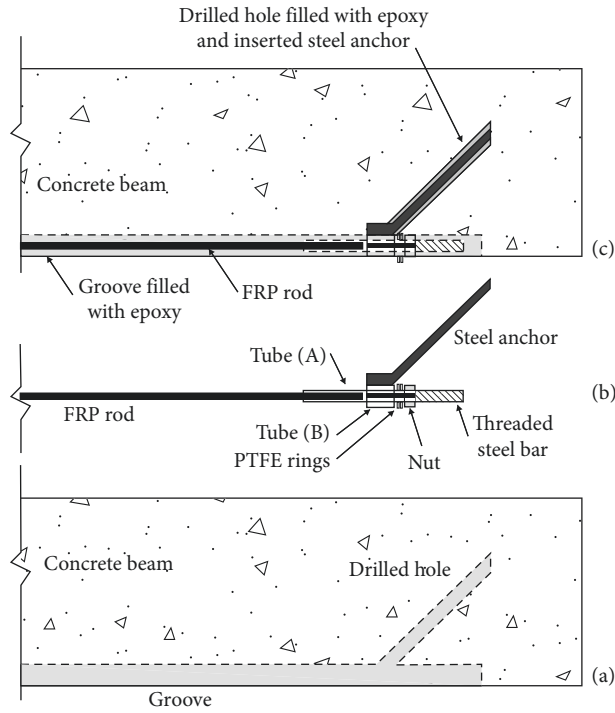
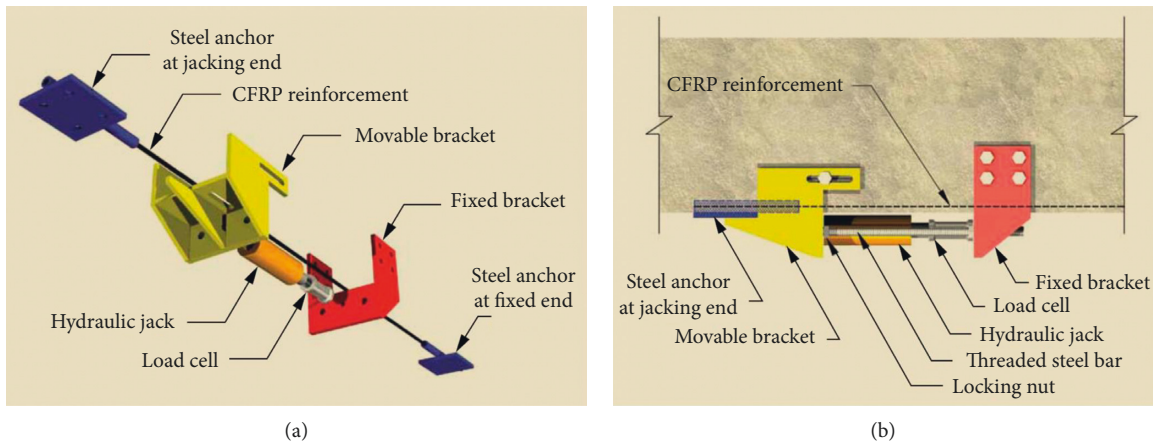FIGURE 7: Installation and setup of anchor proposed by Lecce University [7].

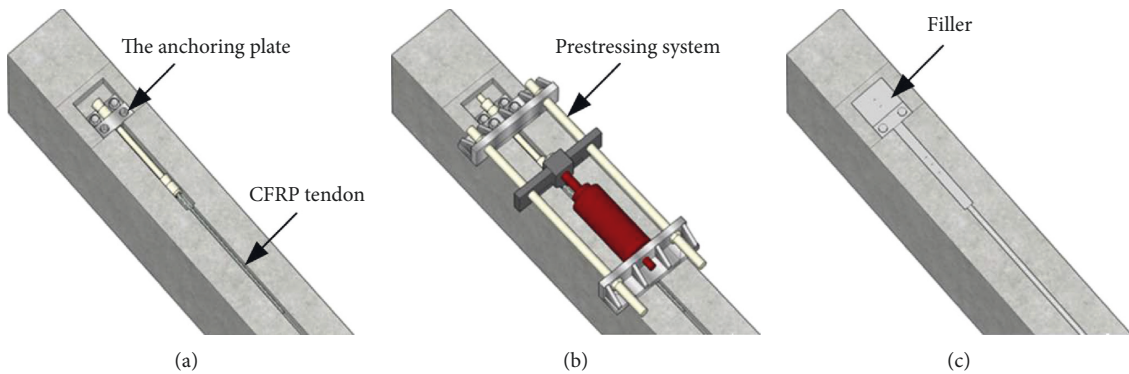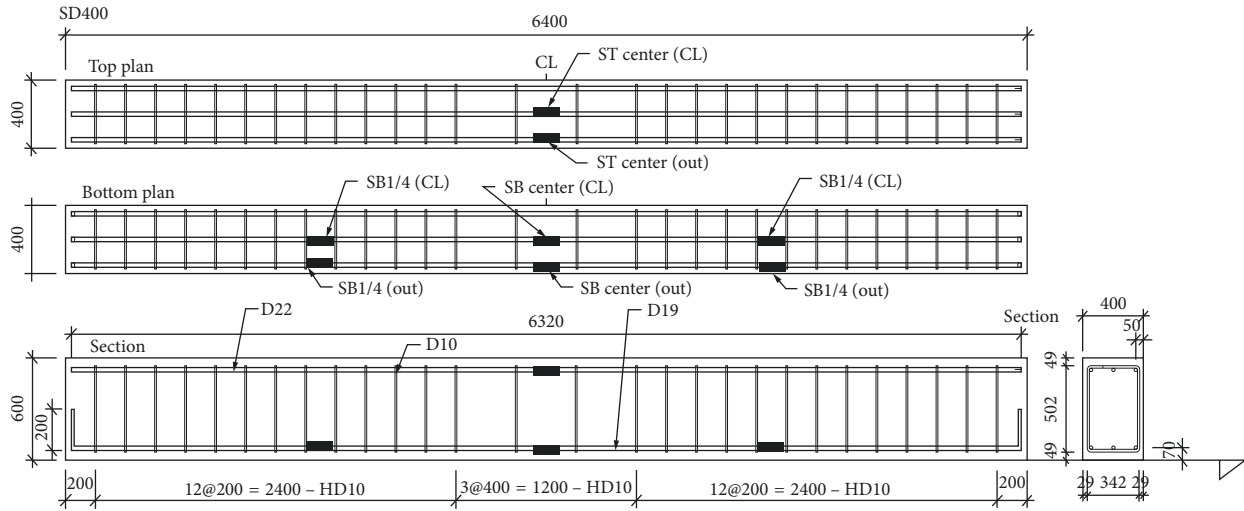FIGURE 8: Anchor proposed by Gaafar [13].

FIGURE 9: KICT anchor [1].
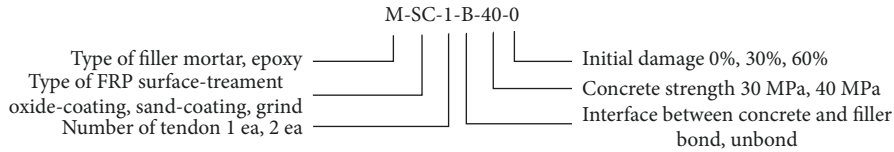
Figure 10: Layout of rebar gauges (in mm).

Figure 11: Designation of specimens.

Table 4: Test variables and designation of specimens.

Group	Designation	Filler type	Surface treatment of tendon	No. of reinforcement	Bonding	f_{ck}(MPa)	Damage ratio w.r.t. Control (%)	Strengthened length (m)
I	Control-1	—	—	—	—	40	—	—
	M-SC-1-B-40-0	Mortar	Sand coating	1	O	40	0	4.8
	M-SC-2-B-40-0	Mortar	Sand coating	2	O	40	0	4.8
	M—GR-1-B-40-0	Mortar	Grind	1	O	40	0	4.8
II	Control-2	—	—	—	—	—	—	—
	E-OX-1-B-40-0	Epoxy	Oxide coating	1	O	40	0	4.8
	E-OX-1-UB-40-0	Epoxy	Oxide coating	1	X	40	0	4.8
	E-OX-1-B-30-0	Epoxy	Oxide coating	1	O	30	0	4.8
	E-OX-1-B-40-30	Epoxy	Oxide coating	1	O	40	30	4.8
	E-OX-1-B-40-60	Epoxy	Oxide coating	1	O	40	60	4.8

Table 5: Physical properties of 10 mm FRP tendon.

Ultimate load (kN)	Tensile strength (MPa)	Median strain at rupture (10^{-6})	Elastic modulus (GPa)
>240	3058.3	17890	171

Surface treatment	Image	Execution time
Grinding		At production
Sand coating		At production
Oxide coating		Manual posttreatment

4.3. Grooving of Indentation. Since the prestressed NSMR requires the CFRP tendon be embedded in concrete, grooves were prepared for the anchoring. The rectangular indentations were grooved with a width of 30 mm and length of 40 mm at the locations indicated in Figure 12.

4.4. Prestressing. The process of prestressed NSMR is illustrated in Figure 13. First, grooving is executed at the bottom of the specimen (Figure 13(a)). The grooves involve those for installing the anchors and the longitudinal ones for the embedment of the CFRP tendons. Anchor holes are drilled as shown in Figure 13(b) for the installation of the anchor in the indentation. Since grooving is done manually, it is difficult to execute horizontally the 40 mm deep groove. Consequently, leveling by epoxy putty is done at places where the anchor is to be installed (Figure 13(c)) before the installation of the anchor (Figure 13(d)). The anchor bolts are then fastened up to the specified torque, and the gap between the anchor and the edge of the groove are filled with epoxy to complete the installation of the anchor (Figures 13(e) and 13(f)). The CFRP tendon is now inserted in the anchor groove at the fixed end considering the stretched length after tensioning, and a washer is used to prevent the slip of the sleeve in the anchor (Figure 13(g)). The opposite side of the so-fastened FRP tendon is finally inserted in the anchor groove of the jacking end and fixed using a nut (Figure 13(f)).

The tensioning of CFRP starts by pushing the swaged-anchored side toward the support by means of a hydraulic cylinder. Here, the swaged-anchored steel sleeve is fastened to an inverted U-shape jig at the bottom of the tensioning system and is pushed in the hole prepared in the jacking end. The prestress force is introduced by a nut fixed to the protruding screw tap.

4.5. Summary of Test and Measurement. The test for the evaluation of the strengthening performance was executed using a 2,000 kN-UTM (universal testing machine). All the specimens were subjected to the 4-point loading flexural test. The loads were applied identically at spots located symmetrically 500 mm far away from the center to secure a pure bending length of 1 m. For the sake of safety, loading was applied through displacement control at a speed of 0.03 mm/s for the first 30 mm and 0.1 mm/s beyond. Rubber pads were installed between the loading jig and concrete to prevent the occurrence of stress concentration. Figure 14 schematically describes the test setup, and Figure 15 shows the actual implemented test.

Strain gauges were attached to the surface of the tendon and concrete to examine the strengthening performance of the prestressed NSMR specimens, and the displacement was installed at important locations to measure the overall behavior. The deflection was measured by means of 3 LVDTs installed at midspan and quarter length of the specimens (Figure 15(a)). The concrete strain was measured in midspan at vertical distances of 50 mm and 100 mm from the top surface and at the top surface on the left- and right-hand sides of the loaded points (Figure 15(b)). In addition, steel gauges were installed at 8 spots to measure the strain of the internal rebar. Steel gauges were also attached at midlength and both quarter lengths of the CFRP tendon.

5. Test Results and Discussion

5.1. Failure and Cracking. The Control specimens in Groups I and II experienced typical flexural failure involving successively cracking, rebar yielding, and concrete crushing as shown in Figure 16. Strengthened performance of the strengthened specimens increased after the yielding of rebar, and the test was completed at rupture of the CFRP tendon around the occurrence of concrete crushing. After the completion of the test, visual observation could not find any trace of cracking at the ends installed with the anchors, nor spalling of the filler.

At the initiation of cracking, cracks appeared in the tension zone of the pure bending section and propagated toward the compression zone and the supports with the increase of the load. Prior to the failure of the specimens, large inclined cracks occurred around the left-hand side support leading to the completion of the test. In the specimens with 60% damage ratio of the matrix concrete, the increase of the load opened the closed cracks and generated more numerous cracks compared to the other specimens. Besides, the specimens with concrete strength of 40 MPa showed slighter cracking than the specimen with 30 MPa. Table 7 summarizes the test results of the specimens of Groups I and II. The static loading data used to support the findings of this study are included within the article.

5.2. Effect of Surface Treatment and Number of FRP Tendon. Figure 17 shows the strengthning effect with regard to the surface treatment. The comparison of the specimens with grinded and sand-coated tendons reveals that there is no significant difference in the crack load and yield load but that the sand-coated specimens provided improvement of the failure load by about 12%. This difference can be attributed to the surface treatment, which is directly linked to the bond strength of the CFRP tendon. Especially, this difference appears to be more acute after the rebar yielding. Consequently, the execution of sand coating can be recommended to improve the bond performance if the tendon has low bond strength.
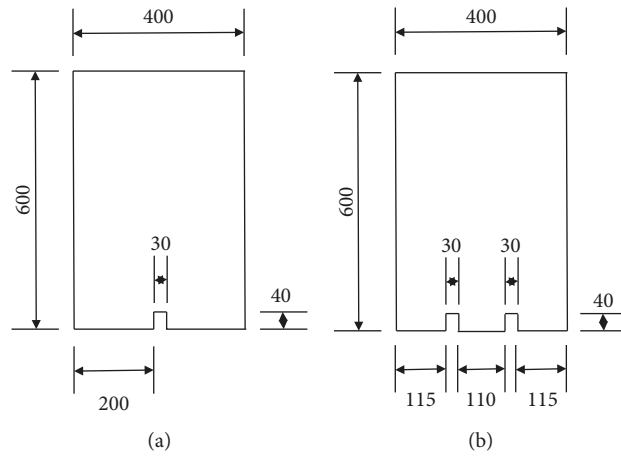
Figure 12: Dimensions of grooves (in mm). (a) One line. (b) Two lines.

Figure 13: Continued.

<center>(g)</center>

<center>(h)</center>

FIGURE 13: Installation process of anchor and FRP tendon. (a) Grooving. (b) Drilling of anchor bolt holes. (c) Leveling of groove by epoxy. (d) Fastening of anchor bolt. (e) Installation of anchor bolt using torque wrench. (f) Installed anchor. (g) Fixation of anchor at the fixed end by washer. (h) Nut fastening of anchor in jacking end.
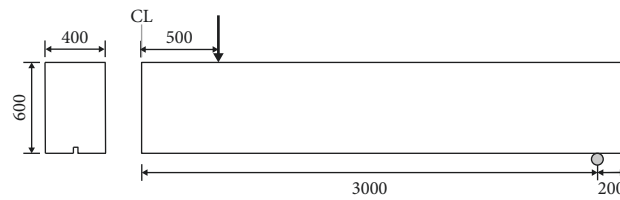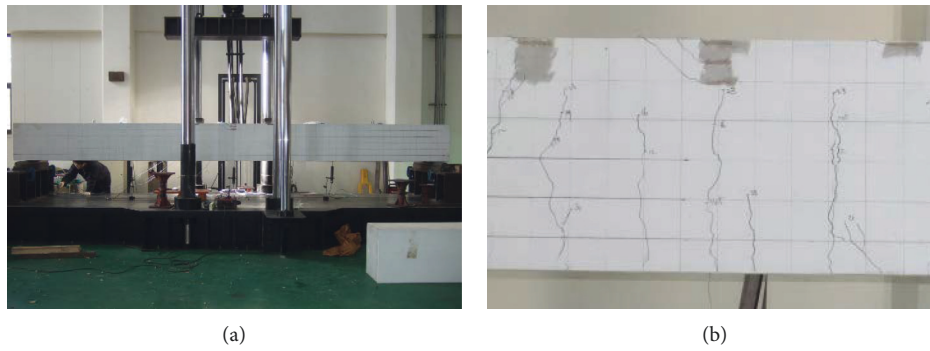

FIGURE 14: Test setup (in mm).

<center>(a)</center>

<center>(b)</center>

FIGURE 15: Loading test. (a) UTM setup. (b) Loaded specimen.

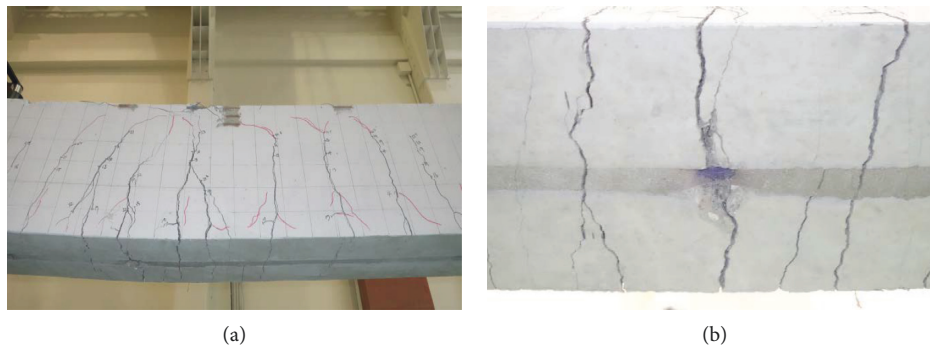

<center>(a)</center>

<center>(b)</center>

FIGURE 16: Tensile failure of strengthened specimen.

The test results with regard to the amount of reinforcement show that, with reference to the nonstrengthened specimen, one line improved the performance by 55% and two lines by 95%. Since two lines strengthening can be installed in the 40 cm wide specimen, it seems that 3 lines can be accommodated by adjusting the disposition of the anchors (Figure 18).

TABLE 7: Summary of test results.

Specimen	Cracking			Yield			Failure			Ductility (D_{max}/D_y)	Failure mode
	Load (kN)	Disp. (mm)	Ratio to Control (%)	Load (kN)	Disp. (mm)	Ratio to Control (%)	Load (kN)	Disp. (mm)	Ratio to Control (%)		
Control-1	68.3	2.5	—	160.1	21.1	—	193.2	105.4	—	5.00	C
M-SC-1-B-40-0	118	4.1	72.77	224.4	22.4	40.16	298.9	84.5	54.71	3.77	F
M-SC-2-B-40-0	143.2	4.6	109.66	283.2	25.2	76.89	379.4	98.9	96.38	3.92	F
M—GR-1-B-40-0	120.9	4.4	77.01	216.7	21	35.35	265.7	86.5	37.53	4.12	F
Control-2	37.61	1.18	—	145.22	20.32	—	175.5	166.59	—	8.20	C
E-OX-1-B-40-0	69.24	2.48	84.10	198.89	22.06	36.96	283.6	141.88	61.60	6.43	F
E-OX-1-UB-40-0	68.36	2.38	81.76	186.52	21.2	28.44	243.15	126.44	38.55	5.96	C, F
E-OX-1-B-30-0	69.53	2.06	84.87	197.57	21.9	36.05	272.74	139.06	55.41	6.35	F
E-OX-1-B-40-30	—	—	—	199.52	21.34	37.39	290.08	122.18	65.29	5.73	F
E-OX-1-B-40-60	—	—	—	201.85	19.86	39.00	274.98	99.72	56.68	5.02	C, F

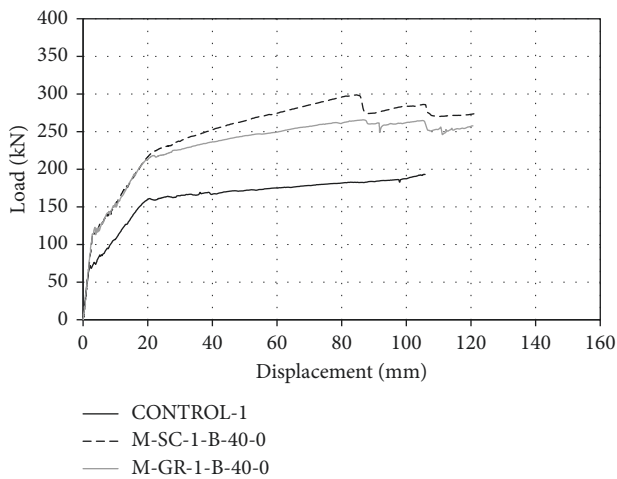*Note.* C = concrete crushing; F = CFRP rupture.

FIGURE 17: Strengthening effect w.r.t. surface treatment.
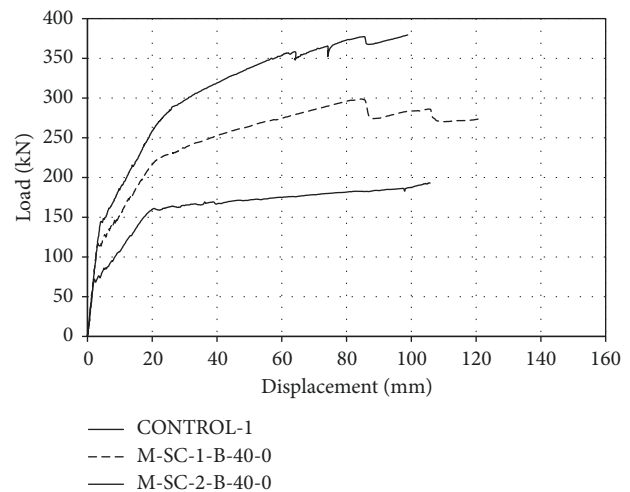

FIGURE 18: Strengthening effect w.r.t. amount of reinforcement.

5.3. Cross-Sectional Strain Distribution.

Figure 19 shows the distribution of the strain per loading stage in the central section of the nonstrengthened and strengthened specimens is presented for the concrete compression zone, tensile reinforcement, and CFRP tendon. The measurements show that the strain after yielding of the tensile rebar does not exhibit linear distribution in most of the strengthened specimens. Especially, the neutral axis did practically not change until the yield load but moved steeply toward the compression zone after yielding.

The strain of the CFRP tendon initially behaved identically to that of the tensile rebar and increased linearly. However, the initiation of cracking shortened the developed length between the CFRP tendon and the filler and provoked local bond failure. This made the tendon strain increase slower than the rebar strain and indicated that monolithic behavior was not secured anymore. Thereafter, the CFRP tendon sustained the stress together with the tensile rebar until yielding. After rebar yielding, local bond failure occurred but the CFRP tendon could develop full performance because the bond of the CFRP tendon and its anchors resisted the external force.

5.4. Strain in CFRP Tendon.

In view of the tensile performance of the CFRP tendon, the strain reached about 18,000 $\mu\varepsilon$ under 240 kN load. Considering that the strain at rupture cannot be measured if the gauge attached to the surface of the tendon breaks before the rupture of the specimen, the strain at rupture can be obtained by linear interpolation from the final strain measured considering the maximum load of the specimen to the rupture of the specimen. Table 8 arranges the so-predicted values of the
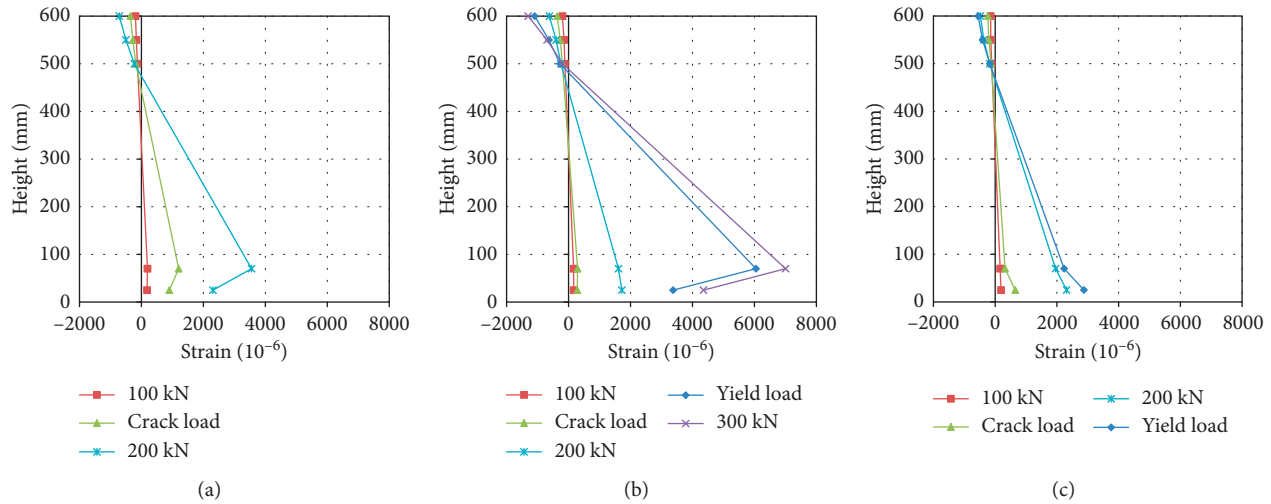
Figure 19: Strain distribution in cross section. (a) M-SC-1-B-40-0. (b) M-SC-2-B-40-0. (c) M-GR-1-B-40-0.

Table 8: Designation of specimens and corresponding test variables.

Variable	FRP strain during prestressing ($\mu\varepsilon$)	Measured final strain ($\mu\varepsilon$)	Predicted final strain ($\mu\varepsilon$)
M-SC-1-B-40-0	7164	15786	19396
M-SC-2-B-40-0	6035	11913	22278
	7579	11631	19539
M-GR-1-B-40-0	8075	13915	17951
E-OX-1-B-40-0	5695	18902	—
E-OX-1-UB-40-0	5200	10728	14528
E-OX-1-B-30-0	6272	17658	—
E-OX-1-B-40-30	6595	15982	19253
E-OX-1-B-40-60	6636	17008	—

rupture strain. All the specimens show fair approximation of the rupture strain of the tendon. It can be seen indirectly that the tendons broke when their tensile strength was reached around the maximum load. However, compared to the bonded specimens, the nonbonded specimen (E-OX-1-UB-40-0) experienced larger increase of the strain at the end of the CFRP tendon and the strain on CFRP tendon developed smaller than the others. This prevented the CFRP tendon to develop fully its tensile performance, generated problems in the anchor sleeve, and resulted in the premature completion of the test. Besides, the bonded specimens saw their CFRP tendon resist until the final tensile strength, thanks to the bond performance of the filler even if the swaged-anchor could not fulfill its performance to the end (Figure 20).

Figure 21 plots the strains measured along the CFRP tendons during the tests. The length of the tendon being 4,800 mm, the strain was measured by 1 gauge disposed at midlength and 2 gauges disposed at quarter length. The horizontal axis of the graphs represents the length of the tendon, and the vertical axis indicates the strain. For each specimen, the strains were measured at crack load, yield load, and at 235 kN. The bonded specimens showed clear increase of the strain at midlength of the tendon according to the increase of the load, whereas the 3 gauges attached to the unbonded specimens exhibited similar increase rate of the strain as shown in Figure 21(b). This indicates that the anchoring performance at the end of the CFRP tendon is critical

in the unbonded specimens because the stress is distributed evenly. The cracks in the bonded specimens initiated at the center and propagated toward the ends. This situation was confirmed by the largest strains measured at the center of the CFRP tendon and by the fact that the stress at the ends of the tendon remained low until the termination of the test.

5.5. Effect of Matrix Concrete Strength. The strength of deteriorated concrete is naturally lower than the design strength. Accordingly, it seems necessary to examine the strengthening effect for the structure with degraded concrete strength. Figure 22 plots the load-deflection curves measured at midspan of the specimens. Both Control specimens and strengthened specimens exhibited typical flexural behavior characterized by the crack load, yield load and maximum load. Compared to the nonstrengthened specimen Control-2, the crack load, yield load, and maximum load of specimen with matrix concrete strength of 30 MPa (E-OX-1-B-30-0) improved, respectively, by 84%, 36%, and 55% and by 84%, 36%, and 61% for the specimen with matrix concrete strength of 40 MPa (E-OX-1-B-40-0). This difference of 10 MPa in the matrix concrete strength appears to have no special effect on the strengthening effect of the prestressed NSMR.

5.6. Effect of Bonding of CFRP Tendon. As shown in Figure 23, compared to Control, the unbonded specimen without epoxy
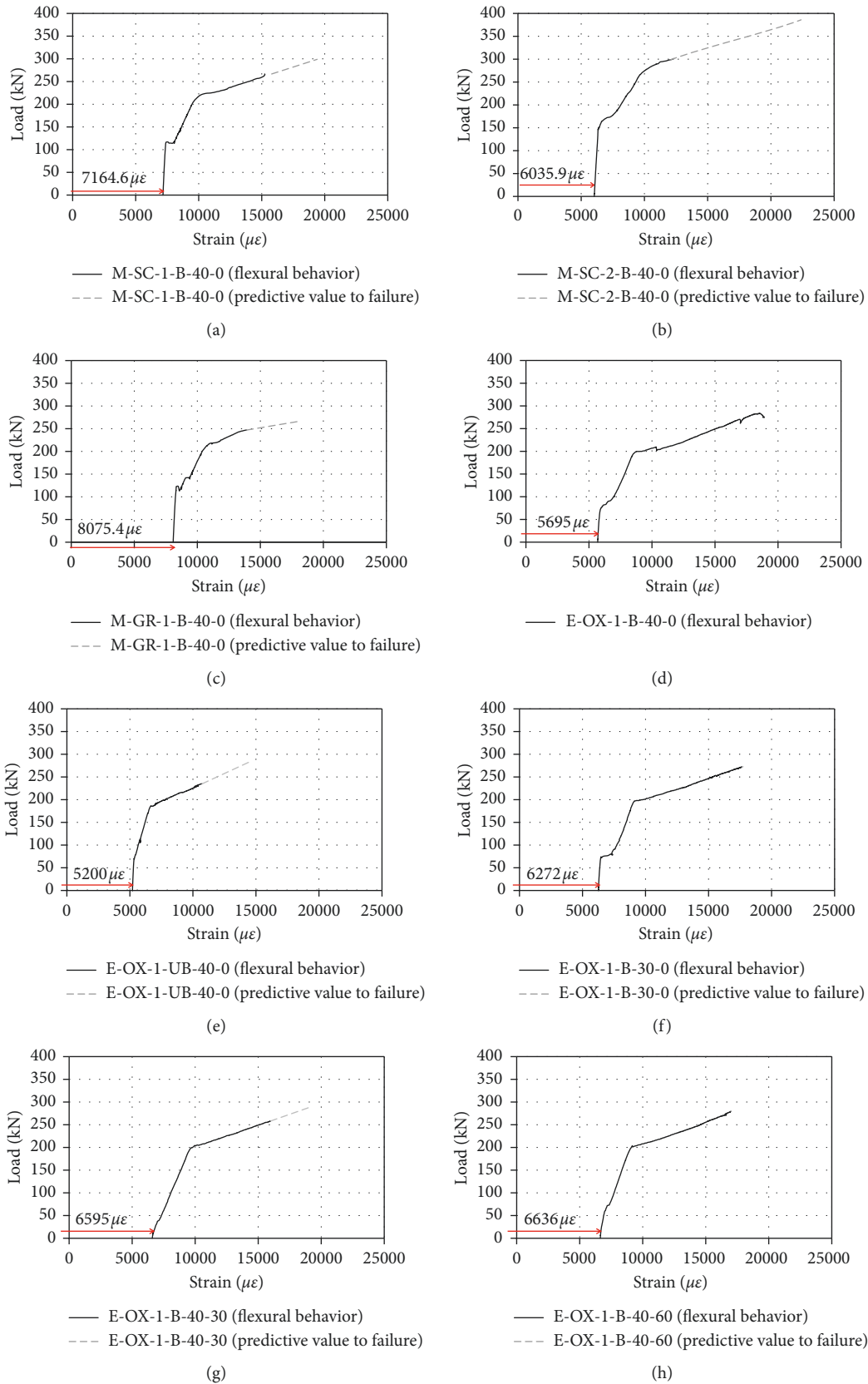
Figure 20: Strain distribution of tendon according to change in post-tension force. (a) M-SC-1-B-40-0. (b) M-SC-2-B-40-0. (c) M-GR-1-B-40-0. (d) E-OX-1-B-40-0. (e) E-OX-1-UB-40-0. (f) E-OX-1-B-30-0. (g) E-OX-1-B-40-30. (h) E-OX-1-B-40-60.
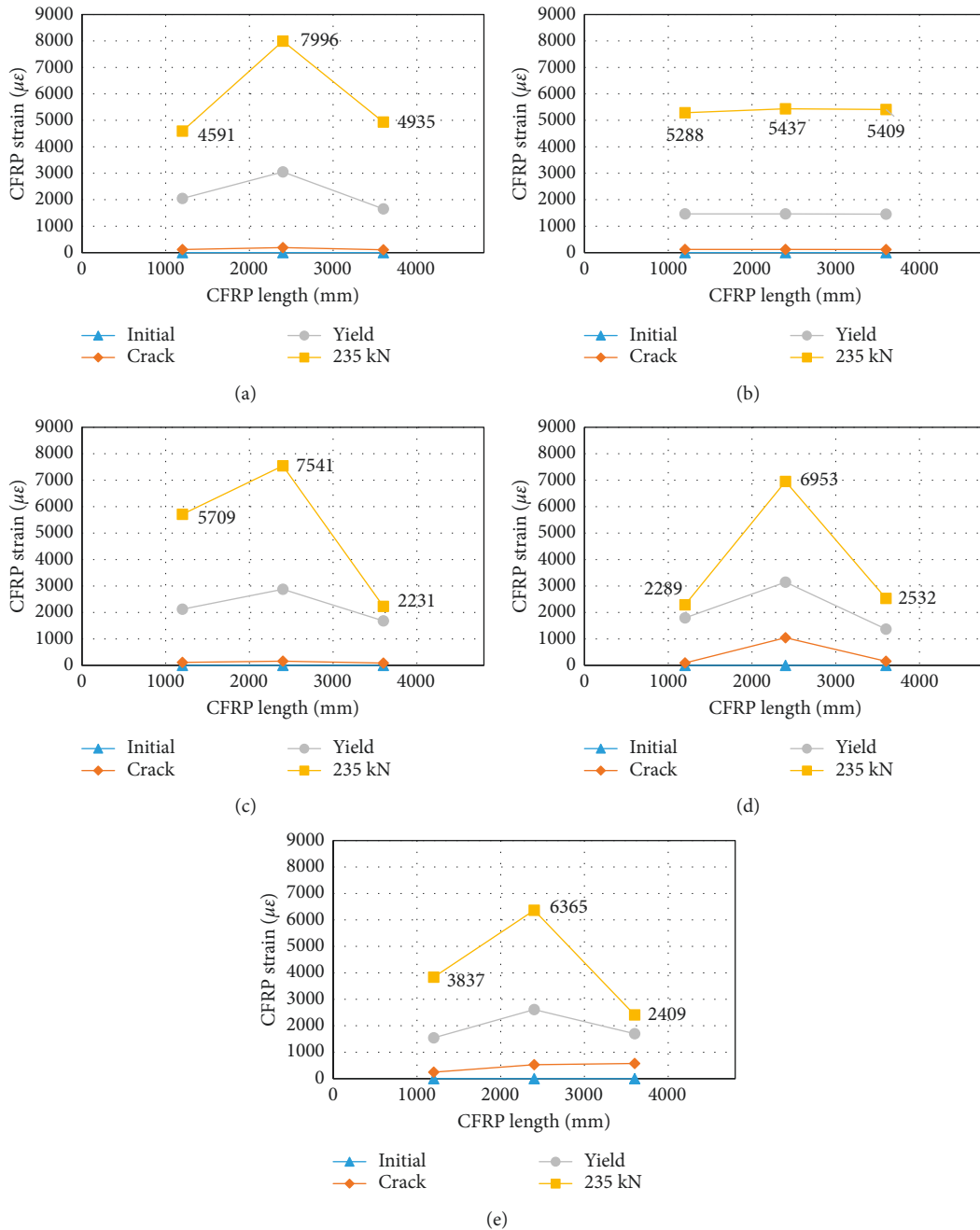
FIGURE 21: Strain distribution of CFRP tendon. (a) E-OX-1-B-40-0. (b) E-OX-1-UB-40-0. (c) E-OX-1-B-30-0. (d) E-OX-1-B-40-30. (e) E-OX-1-B-40-60.

filling (E-OX-1-UB-40-0) developed enhanced performance with an increase of the crack load by 81%, yield load by 28%, and maximum load by 38%. Similarly, the bonded specimen with epoxy filling (E-OX-1-B-40-0) secured enhanced crack load by 84%, yield load by 36%, and maximum load by 61% compared to Control. Even if the unbonded specimen showed similar behavior to that of the unbonded specimen before the yielding of the rebar, the absence of epoxy lowered its sectional stiffness after the rebar yielding and provided less strengthening effect than the bonded specimen. Compared to the unbonded specimen (E-OX-1-UB-40-0), the bonded specimen (E-OX-1-

B-40-0) developed crack load, yield load, and maximum load larger by 16%, 10%, and 17%, respectively. It appears that the epoxy filling improved the performance at each loading stage. Consequently, the bonding of the CFRP tendon and concrete by a filler is necessary for the improvement of the strengthening performance.

5.7. Flexural Behavior with Concrete Damage. Concrete structures degrade due to diverse factors and may experience loss of their performance. With regard to this observation,
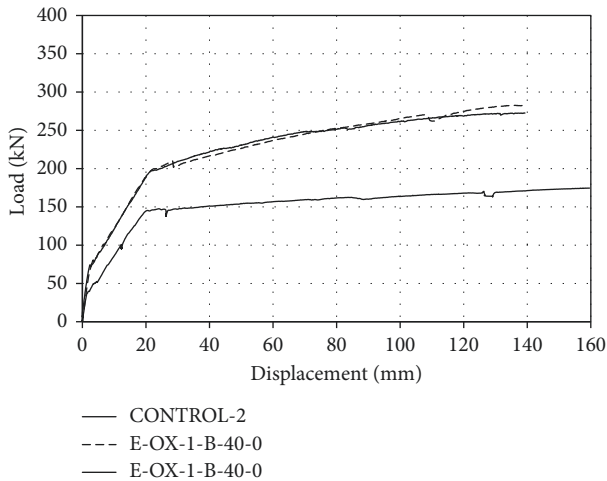
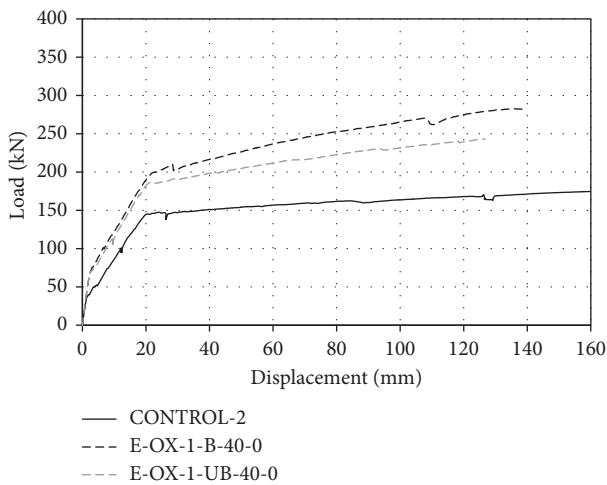Figure 22: Strengthening effect w.r.t. matrix strength.

Figure 24: Strengthening effect w.r.t. damage extent of matrix.

Figure 23: Strengthening effect w.r.t. eventual bonding of tendon.
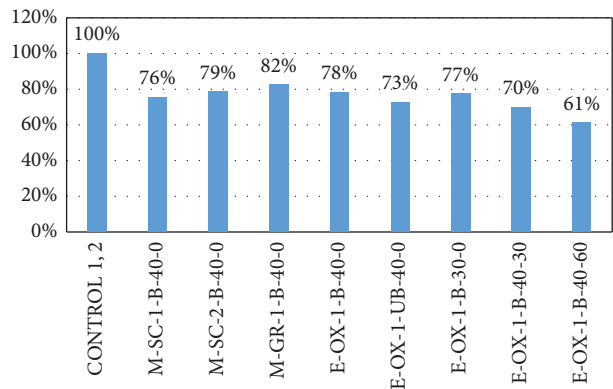
Figure 25: Ductility of developed prestressed NSMR.

degraded specimens were simulated by applying preliminary load up to 30% and 60% of the maximum load to the nonstrengthened specimens. These degraded specimens were then strengthened and their respective strengthening effect was examined with respect to the degree of damage.

Compared to Control, the specimen with 30% damage ratio of the matrix concrete (E-OX-1-B-40-30) developed performance improved by 37% for the yield load and 65% for the maximum load, and the specimen with 60% damage ratio of the matrix concrete (E-OX-1-B-40-60) achieved yield load and maximum load improved by 39% and 56%, respectively. For the strengthened specimens in which cracking was induced by preliminary loading, there was no crack load, and the specimens behaved linearly until the yield load. Beyond the yield load, these specimens behaved similarly to the other strengthened specimens. Compared to Control, the damaged specimens E-OX-1-B-40-30 and E-OX-1-B-40-60 presented improvement of all loading stages and presented similar behavior to that of the un-damaged specimen E-OX-1-B-40-0. Accordingly, the strengthening of degraded concrete structures by the
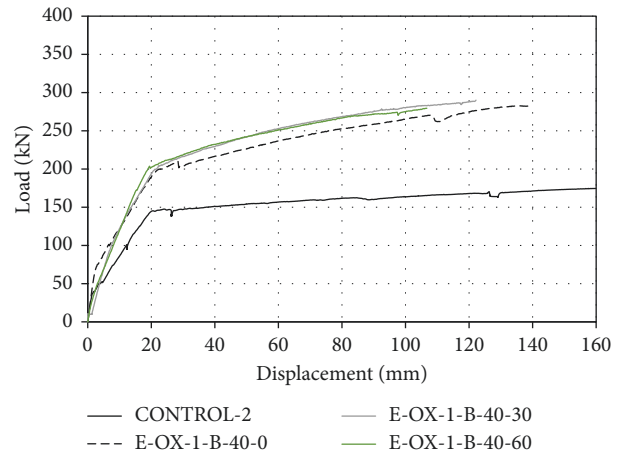
prestressed NSMR appears to enable not only recovery but also improvement of the original performance (Figure 24).

5.8. *Ductility.* The ductility of the prestressed NSMR specimens tends to diminish compared to that of the structure before strengthening. Here, the ductility is defined as the ratio of the deflection at failure to the deflection at yielding (D_{max}/D_y). Report stated that, in general, the ductility tends to reduce by about 45% when prestressed NSMR is applied using CFRP tendon with large bond strength [17]. The analysis of the ductility of the strengthened specimens reveals that the ductility loss was less than 30% (Figure 25). This lesser loss of the ductility compared to the previous literature can be explained by the occurrence of local failure between the CFRP tendon and the filler after the yielding of the rebar, thanks to the bond strength of the CFRP tendon. Especially, the grinded specimen with low bond strength (M-GR-1-B-40-0) developed a ductility that improved by about 9% compared to the sand-coated specimen (M-SC-1-B-40-0). In the absence of bond, failure occurs because the anchoring performance of the CFRP tendon is overwhelmed in the anchor, and the loss of ductility reaches approximately 7%. Consequently, it
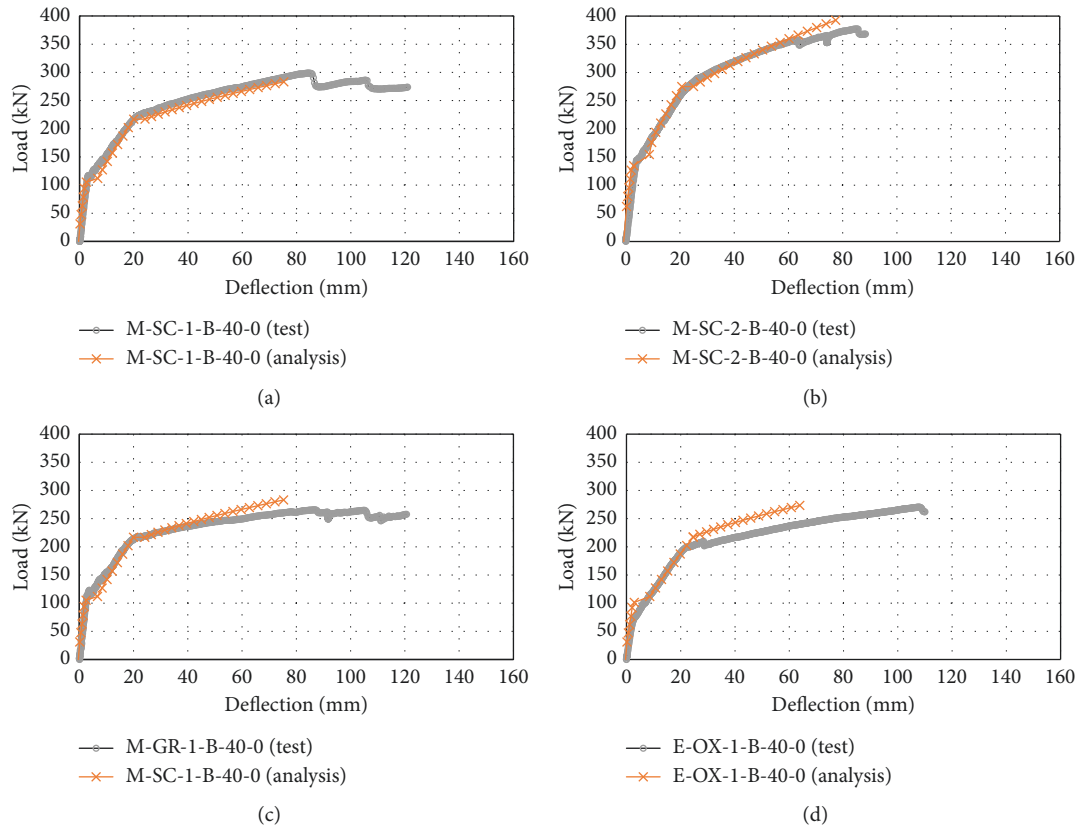
Figure 26: Measured load-strain curves. (a) M-SC-1-B-40-0. (b) M-SC-2-B-40-0. (c) M-GR-1-B-40-0. (d) E-OX-1-B-40-0.

appears that the filler is indispensable to secure stable ductile behavior. For the degraded specimens with damaged matrix (30% and 60% damage), the ductility was lower, respectively, by 10% and 20% compared to the strengthened specimen without damage. This indicates that the ductility lowers as much as the matrix concrete damage is large.

5.9. Comparison with Analytical Results. Several researchers proposed bond failure models to predict the behavior of the NSMR specimen. However, there is no need for complex bond failure model to analyze the behavior of the prestressed NSMR specimen because this strengthening allows the CFRP tendon to develop fully its material performance [18–20]. Accordingly, this study adopts the sectional analysis based upon the strain compatibility and the force equilibrium to predict the behavior of the prestressed NSMR beam.

The moment-curvature distribution of the conventional reinforced concrete member can be divided into 3 parts with reference to the initiation of concrete cracking and the yielding of rebar. Therefore, the sectional analysis also considers 3 levels of the moment resulting from the load. The computational process is as follows. When the strain is increased, the load is calculated by means of the strain compatibility, the constitutive equations of each material, and the internal equilibrium to determine the position of the neutral axis, the strain of each material, and the deflection. For the decision of the final failure mode, compressive failure of concrete occurs when the compressive strain of the top

concrete exceeds 0.003 and rupture of the tendon is assumed when the rupture strain of the CFRP tendon is exceeded.

Figure 26 compares the analytical and experimental values according to the amount of reinforcement and type of surface treatment. The results of the analysis in Figures 26(a) and 26(b) show that the maximum load is predicted within an error of 7%. The smaller slope of the experimental curve can be attributed to the occurrence of cracks in the top concrete. The drop of the postyield bond strength observed in Figure 26(c) comparing the results with respect to the surface treatment of the tendon may be explained by the lowering of the slope because of the loss of the bond between the tendon and the filler. In Figure 26(d) related to the oxide coating, the lowering of the slope is due to the loss of bond strength caused by defective coating.

6. Conclusions

This study examined the flexural behavior of specimens strengthened by prestressed NSMR using CFRP tendon considering diverse variables. The following conclusions can be drawn based on the tests performed.

Compared to the nonstrengthened member, the performance was improved by about 55% when one line was used and by 96% when two lines were used. Since two lines strengthening could be achieved in the 400 mm-wide specimen, 3 lines can also be accommodated by adjusting the disposition of the anchors.

The specimens in which the CFRP tendon was bonded by a filler showed a clear increase of the strain measured at a midlength of the tendon with a larger load. Besides, the specimens in which the tendon was not bonded presented a similar increase rate of the strain at each loading stage. This indicated the importance of the anchoring performance at the extremity of the unbonded tendon because of the even distribution of the stress along the tendon.

The cracks in the specimens with bonded tendon initiated at the center and propagated toward the ends. This situation was confirmed by the largest strains measured at the center of the CFRP tendon and by the fact that the stress at the ends of the tendon remained low until the termination of the test.

The bond of the CFRP tendon achieved by the epoxy filling provided improved performance at all loading stages. Accordingly, the bond of the CFRP tendon with concrete by means of the filler appeared to be necessary for the improvement of the strengthening performance. The strengthening of degraded concrete structures by the prestressed NSMR enabled not only recovery but also improvement of the original performance.

The strengthened specimens experienced loss of the ductility compared to the nonstrengthened specimen. The ductility was seen to depend on the presence or not of the filler, the surface treatment of the CFRP tendon, and the degree of damage of the matrix concrete. In addition, the use of a filler was necessary to secure stable ductile behavior, and stronger damage decreased the ductility. Therefore, the loss of load bearing capacity should be considered when strengthening the structure.

The sectional analysis could predict the maximum load of the reinforced concrete beam strengthened by prestressed NSMR within an error of 7%. However, considering the dependence of the deflection on the bond performance of the CFRP tendon, surface treatment appeared to be necessary for improving the strengthening performance.

Data Availability

The data used to support the findings of this study are included within the article.

Conflicts of Interest

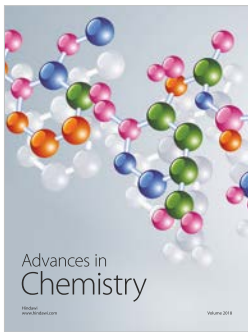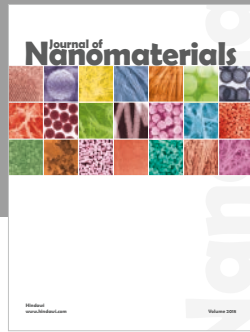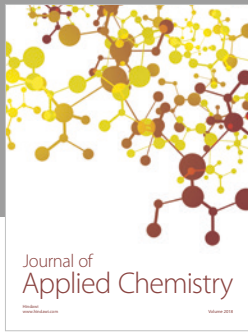The authors declare that they have no conflicts of interest.

Acknowledgments

References

[1] KICT, "Development of bridge strengthening methods using prestressed FRP composites," Tech. Rep., KICT, Korea, 2015.

[2] ACI 440.3R-04, *Test Methods for Fiber-Reinforced Polymers (FRPs) for Reinforcing or Strengthening Concrete Structures*, American Concrete Institute, Farmington Hills, MI, USA, 2004.

[3] A. Nanni, C. E. Bakis, E. F. O'Neil, and T. O. Dixon, "Performance of FRP tendon-anchor systems for prestressed concrete structures," *PCI journal*, vol. 41, no. 1, pp. 34–44, 1996.

[4] ACI 440.4R-04, *Prestressing Concrete Structures with FRP Tendons*, American Concrete Institute, Farmington Hills, MI, USA, 2004.

[5] A. Bennitz, "Mechanical anchorage of prestressed CFRP tendons—theory and tests," Licentiate Thesis, Luleå University, Luleå, Sweden, 2008.

[6] W. T. Jung, Y. H. Park, and J. S. Park, "An experimental study on improving anchor performance for CFRP tendons," in *Proceedings of the 10th International Symposium on Fiber Reinforced Polymer Reinforcement for Concrete Structures (FRPRCS-10)*, pp. 41.1–41.15, Tampa, FL, USA, April 2011.

[7] R. El-Hacha and K. Soudki, "Prestressed near-surface mounted fibre reinforced polymer reinforcement for concrete structures—a review," *Canadian Journal of Civil Engineering*, vol. 40, no. 11, pp. 1127–1139, 2013.

[8] H. Lee, W. T. Jung, and W. Chung, "Bond behavior of near surface mounted CFRP rods under temperature cycling," *Engineering Structures*, vol. 137, pp. 67–75, 2017.

[9] H. Lee, W. Lee, W. T. Jung, and W. Chung, "Bond characteristics of near-surface-mounted anchorage for prestressing," *Construction and Building Materials*, vol. 148, pp. 748–756, 2017.

[10] Y. J. Kim, J. Y. Kang, J. S. Park, and W. T. Jung, "Functional performance of bridge girders strengthened with post-tensioned near-surface-mounted carbon fiber-reinforced polymer," *ACI Structural Journal*, vol. 113, no. 2, pp. 239–250, 2016.

[11] ACC, *Seihin Full from ACC*, ACC Catalog, Japan, 2013.

[12] A. Borosnyói, "Serviceability of CFRP prestressed concretebeams," Ph.D. thesis, Budapest University of Technology, Budapest, Hungary, 2002.

[13] M. Guadagnini, K. Pilakoutas, P. Waldron, and Z. Achillides, "Tests for the evaluation of bond properties of FRP bars in concrete," in *Proceedings of Second International Conference on FRP Composites in Civil Engineering*, pp. 343–350, Adelaide, Australia, December 2004.

[14] M. Badawi, "Monotonic and fatigue flexural behaviour of RC beams strengthened with prestressed NSM CFRP rods," Ph.D. Thesis, University of Waterloo, Waterloo, ON, Canada, 2.

[15] L. De-Lorenzis, F. Micelli, and A. La Tagola, "Passive and active near-surface mounted FRP rods for flexural strengthening of RC concrete beams," in *Proceedings of the 3rd International Conference on Composites in Infrastructure*, San Francisco, CA, USA, June 2002.

[16] R. El-Hacha and M. Gaafar, "Flexural strengthening of reinforced concrete beams using prestressed NSM CFRP bars," *Prestressed Concrete Institute Journal*, vol. 56, no. 4, pp. 134–151, 2011.

[17] KICT, *Development and Application of FRP Prestressing Tendon and Anchorage for Concrete Structures*, Construction & Transportation R&D Report, KAIA, Korea, 2008.

[18] W. T. Jung, J. S. Park, J. Y. Kang, M. S. Keum, and Y. H. Park, "Flexural behaviour of RC beams strengthened with prestressed CFRP NSM tendon using new prestressing system," *International Journal of Polymer Science*, vol. 2017, Article ID 1497349, 9 pages, 2017.

[19] W. T. Jung, Y. J. Kim, J. Y. Kang, and J. S. Park, "State-of-the-practice of constructed bridges in Korea," *Proceeding of the Institution of Civil Engineers Structures and Building*, vol. 171, no. 9, pp. 705–718, 2018.

[20] W. T. Jung, J. S. Park, J. Y. Kang, and M. S. Keum, "Flexural behavior of concrete beam strengthened by near-surface mounted CFRP reinforcement using equivalent section model," *Advances in Materials Science and Engineering*, vol. 2017, Article ID 9180624, 16 pages, 2017.